ORIGINAL PAPER

The effect of vanadium micro-alloying on the microstructure of welded joints in high-strength structural steels

Giulia Stornelli[1] · Anastasiya Tselikova[2] · Rolf Schmidt[2] · Bryan Ramiro Rodriguez Vargas[1] · Guido Zucca[3] · Andrea Di Schino[1]

Abstract

The balance between high strength and toughness in high-strength-low-alloy (HSLA) steels can be defined by the thermal cycles in the heat-affected zone (HAZ) of a welded joint, during a double-pass welding process with secondary heating in the inter-critical zone (IC CG HAZ). After multiple heating cycles in the temperature range between Ac_1 and Ac_3, the steel undergoes a strong loss of toughness and resistance to fatigue, mainly caused by the formation of residual austenite (RA). This study aims to investigate the influence of vanadium addition on the behavior of IC GC HAZ in S355-grade HSLA steel. The welding thermal cycles were simulated, considering five different inter-critical temperatures, between 720 and 790 °C. The addition of vanadium as a micro-alloy to an S355 structural steel was found to increase the mechanical strength of the IC GC HAZ zone of a welded joint without compromising toughness and fatigue resistance. This result is obtained through the generation of a bainitic microstructure with dispersion of fine regions of residual austenite and a fine and uniformly distributed precipitation.

Introduction

In recent years, the use of vanadium as a micro-alloying element has played an important role in the development of high-strength-low-alloy (HSLA) steels, due to its thermodynamic and kinetic ability to form carbides and nitrides [1]. The development of HSLA steels has made possible an innovative and more economically sustainable design also aimed at the most diverse applications [2–5]. Although the use of micro-alloying elements has a fundamental role in improving the strength and toughness of the steel, there are however results in the literature that show an evident decay of the properties in the welded joints [6]. As a result, the use of micro-alloying elements has been severely restricted in the welded component industry. The balance between mechanical strength and toughness in welding HSLA steels

depends on the thermal cycles to which the material is subjected during the welding process. Studying how the addition of micro-alloying elements affects the microstructure and properties of welded joints is quite complex as the set of metallurgical phenomena involved is wide and depends on the chemical composition of the steel and on the conditions of the welding process [7]. Historically, the lowest toughness was expected in the grain-coarsened heat-affected zone (CG HAZ), which is the part of the HAZ closest to the melting line of the weld [8, 9].

However, in recent years, it has been found that the most degraded part is the inter-critically reheated coarse-grained heat-affected zone (IC GC HAZ), which is the region of the GC HAZ heated to temperatures between Ac_1 and Ac_3 by successive welding steps [10]. During the inter-critical thermal cycle, in multi-pass welding there is a partial transformation into austenite which, during cooling, can transform into pearlite/bainite or residual austenite (RA) [11]. The presence of RA is generally considered to be the main factor in reducing the toughness in HAZ [12]. However, the loss of toughness is not only related to the presence of the RA phase but also to its distribution and morphology and to the microstructure of the matrix [13]. Historically, niobium is the most commonly adopted element to improve the strength of HSLA steels. However, it should be specified that in the

✉ Andrea Di Schino
andrea.dischino@unipg.it

1 Dipartimento di Ingegneria, Università degli Studi di Perugia, Via G. Duranti 93, 06125 Perugia, Italy

2 Vantage Alloys AG, Zug, Switzerland

3 Italian Air Force - Aeronautical and Space Test Division, Via Pratica di Mare 45, 00040 Pomezia, Italy

case of niobium as a micro-alloying element, the beneficial effects (grain refinement and improvement of the mechanical properties) are compensated by the negative effects due to the formation of martensite during the welding process with a consequent negative impact on the toughness [14]. Unlike niobium, vanadium has a different effect on the HAZ. It is known that vanadium can refine grain and improve precipitation hardening in HSLA steels, reducing the size of bainitic colonies and promoting nucleation of acicular ferrite [15]. However, to date, the influence of vanadium on the mechanical strength of the IC GC HAZ has not been fully understood and requires further investigation in light of recent developments. This study aims to investigate how the addition of vanadium affects the microstructure and mechanical properties of the IC GC HAZ in S355 steel (EN10025-2), up today considered the standard grade for wind tower application and therefore especially calling for fatigue strength.

Materials and methods

The chemical composition of the steels analyzed in this work is shown in Table 1.

Taking as reference material an industrially produced 16-mm-thickness steel plate in S355 steel for structural applications (EN10025-2), three steel variants were produced through a vacuum induction melting plant (VIM) in the form of 80-kg ingots. These ingots were then hot rolled in a pilot plant to a thickness of 16 mm. The chemical composition of the steels was designed to ensure weldability, considering a $C_{eq} < 0.42\%$ maximum recommended C_{eq} according to the IIW formulation [16]. Starting from the hot-rolled material, cylindrical samples (10 mm long, 4 mm diameter) were obtained and heat treated under controlled conditions using a dilatometer to simulate the IC GC HAZ in a double-pass weld, under different inter-critical conditions. The thermal cycles considered include two heating and cooling cycles:

- First welding cycle: heating from room temperature to 1000 °C with a heating rate of 100 °C/s, holding for 3 s, and cooling to 150 °C with a profile which guarantees a cooling time between 800 and 500 °C (t8/5) about 25 s.

- Second welding cycle: heating from 150 °C to inter-critical temperature (between Ac_1 and Ac_3) with a heating rate of 100 °C/s. The temperatures Ac_1 and Ac_3 were defined by means of a dilatometric test and assumed equal to 715 °C and 815 °C for all the steel variants [17]. The peak temperatures analyzed in the inter-critical zone were 720 °C, 735 °C, 750 °C, 775 °C, and 790 °C, for all variants.

After simulating the welding thermal cycles, the samples for all steel variants were machined, polished, and etched with a 2% Nital solution for 20–40 s. Vickers hardness test were carried out by means of a HV50 (Remet) instruments using a load of 10 kg. The microstructure was then analyzed using an optical microscope (Eclipse LV150 NL, Nikon) and Electron-Backscattered Diffraction (EBSD) with the aim to detect the presence of RA, using a scanning electron microscope with a field emission beam (FEG-SEM) (Ultra-Plus Carl-Zeiss-Oberkochen) equipped with an EBSD detector (C-Nano Oxford Instruments), using a scan step size of 0.1 mm. In addition, by transmission electron microscope (TEM) on extraction replica samples, precipitation state analyses were performed on the alloying variants. Finally, for each variant the mechanical behavior following a welding thermal cycle with an inter-critical temperature of 735 °C was evaluated. The double-pass welding cycles were replicated, using Gleeble, on samples for tensile and fatigue tests. Fatigue tests were conducted on a vibraphone with push–pull configuration, considering fatigue stress loads of 80%, 60%, 40%, 30%, and 20% of the nominal UTS according to the standard.

Results and discussion

The hardness dependence on the inter-critical temperature is shown in Fig. 1 for all variants, compared with the values of the material in the initial state (hot rolled shown with dashed lines). As expected, after the welding thermal cycle, for each steel variant there is an increase in the hardness value compared to the hot-rolled state. While the reference material appears independent of the tested temperature, the Variant I is subject to a loss of hardness. Instead, for Variant II (0.10 wt% V) and Variant III (0.03-wt% V–0.02-wt% Nb) as the inter-critical temperature increases, the hardness decreases, showing a clear micro-alloying effect. In particular, both for Variant II and for Variant III, a peak of hardness at 735 °C is evident and the nature of this behavior can be attributed to various factors, such as the presence of different microstructures, the formation of RA, and/or a different state of precipitation. Strengthening of the steel associated with the formation of RA would be detrimental in terms of toughness [12]. Otherwise, an adequate state of precipitation (fine

Table 1 Chemical composition of the considered steel variants (Fe to balance)

	C wt%	Mn wt%	V wt%	Si wt%	Nb wt%
Reference material	0.16	1.45	–	0.03	–
Variant I	0.16	1.45	0.05	0.03	–
Variant II	0.16	1.45	0.10	0.03	–
Variant III	0.16	1.45	0.03	0.03	0.02

Fig. 1 Effect of the inter-critical temperature on Vickers hardness for the four steel variants; data from [17]
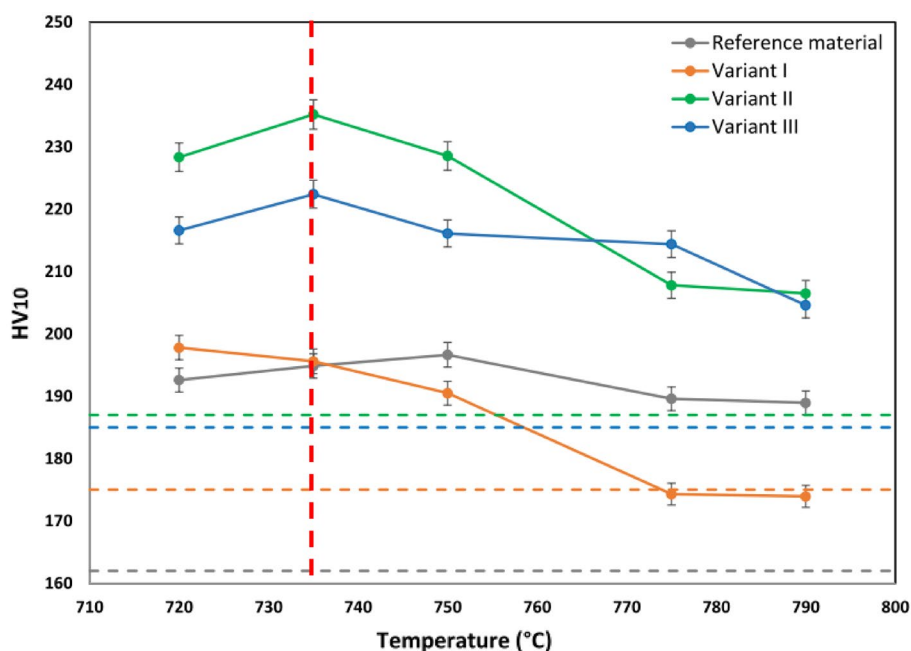
and homogeneously dispersed precipitates) would ensure strengthening and, at the same time, better fatigue resistance [18]. Therefore, the analysis of these metallurgical aspects was performed on selected samples corresponding to the highest hardness values, according to Fig. 1, to focus on the most critical aspects for toughness and fatigue resistance.

Figure 2 shows the microstructural analysis relating to each of the four steel variants following a welding thermal cycle with an inter-critical temperature of 735 °C. The results show that the addition of micro-alloying elements (V or V–Nb) does not lead to any microstructural changes. For the peak temperature of 735 °C, the microstructure appears to be predominantly bainitic for all four variants. Furthermore, as reported in a previous work [17], passing from an inter-critical temperature of 720 °C to 790 °C, the microstructure changes from bainite to ferrite-pearlite, independently from the chemical composition.

EBSD results also show how the amount of residual austenite increases as the content of micro-alloying elements increases. It is anyway to be mentioned that the highest RA measured value is 0.6%, too low to promote detrimental effects on toughness [17]. Furthermore, this increase in RA content was observed regardless of the inter-critical temperature [17, 19, 20].

The analysis of the EBSD data in terms of characterization of the grain boundary typology (High-Angle Grain Boundaries (HAGBs) % with $\phi > 10°$) is shown in Fig. 3. The results show that variant II (0.10 wt% V) has the highest fraction of HAGBs compared to the other variants. This result suggests that this variant is the most promising in terms of mechanical strength (toughness and fatigue

strength), being these edges responsible for a higher crack deflection during propagation [21].

In regard to precipitation state, the scenario was different for Variant II (0.10 wt% V) and Variant III (0.03-wt% V and 0.02-wt% Nb). The size distributions of the precipitates are shown in Fig. 4. The results indicate that for variant II (Fig. 4a), the V-rich precipitates have a size of less than 60 nm, of which more than 50% have an average size of less than 15 nm. This evidence suggests that the addition of vanadium does not appear to have a critical impact on fatigue strength, contrary to what would be expected in the presence of larger precipitates [22, 23]. On the other hand, variant III (Fig. 4b) shows a different precipitation behavior: vanadium is always present in combination with niobium in the precipitates with a maximum size of 90 nm, while the larger precipitates (up to 250 nm) are rich only in Nb. Furthermore, only 30% of Nb–V precipitates are below 15 nm, indicating that the combination of V and Nb micro-alloys could compromise the fatigue performance of a weld joint.

The mechanical behavior of the above microstructures was assessed in term of tensile and fatigue tests. The stress–strain curves for the four steel variants subjected to the double-pass welding thermal cycle with a second peak at the inter-critical temperature of 735 °C are shown in Fig. 5a and the results obtainable from them are summarized in Table 2 in terms of yield stress (YS) and ultimate tensile stress (UTS). Furthermore, in Fig. 5b, the results of the fatigue tests are reported. The results show that, as the vanadium content increases, the combination of a bainitic microstructure, the presence of residual austenite and fine precipitates, and the high fraction HAGBs in the matrix
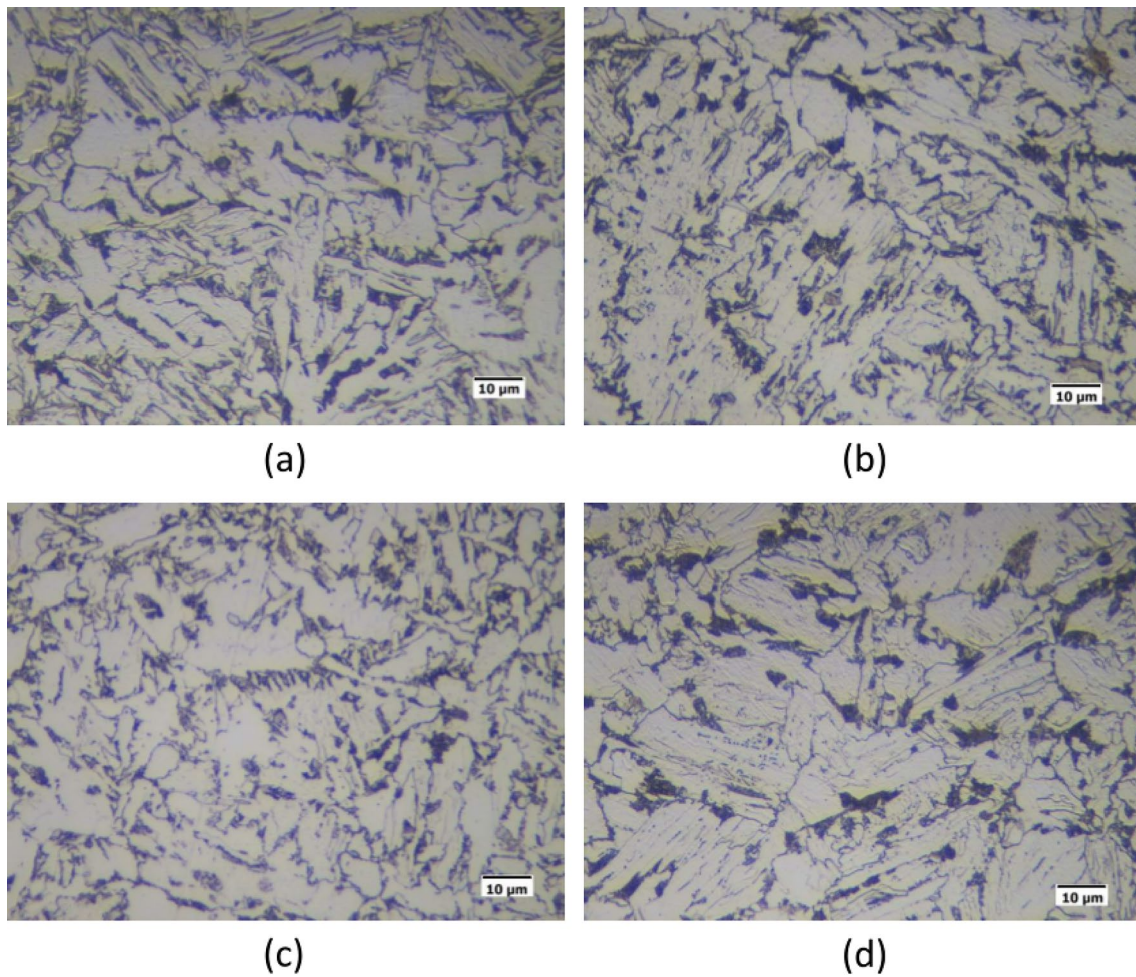
Fig. 2 Microstructure analysis of all steel variants following an inter-critical heat treatment with a second peak temperature of 735 °C: **a** reference material, **b** variant I, **c** variant II, and **d** variant III

Fig. 3 Percentage of high-angle grain boundaries (HAGBs% with $\phi > 10°$) for all steel variants following an inter-critical heat treatment with a second peak temperature of 735 °C
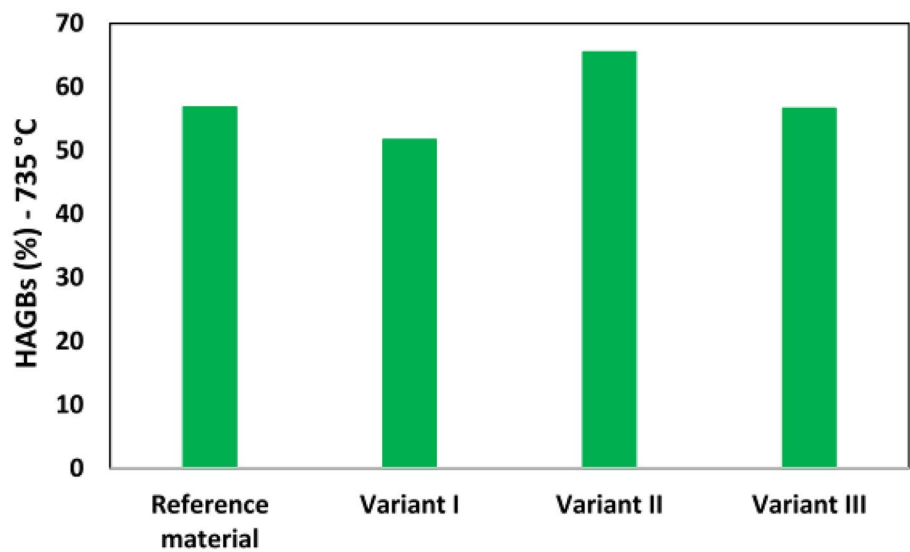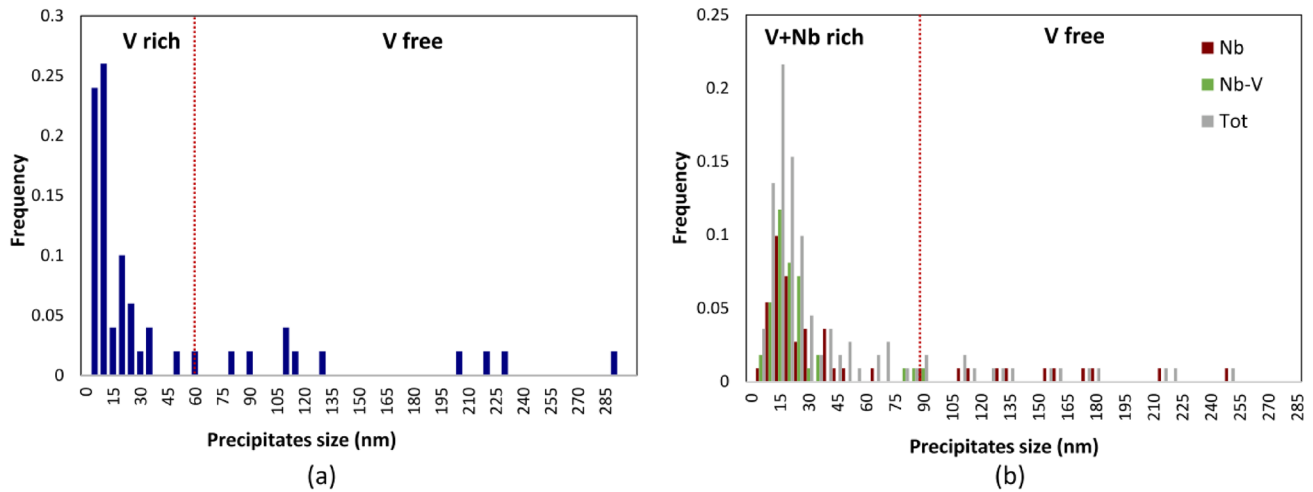
Fig. 4 Size distribution of the precipitates. **a** Variant I and **b** variant III
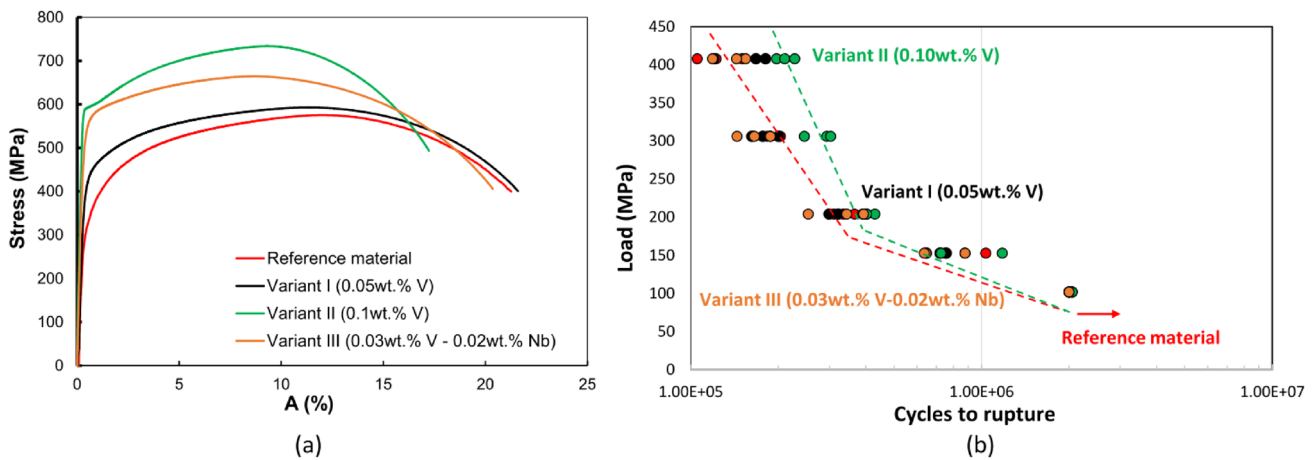
Fig. 5 Stress–strain curve (**a**) and fatigue resistance curve (**b**) of all steel variants following an inter-critical heat treatment with a second peak temperature of 735 °C

Table 2 Mechanical properties of all steel variants following an inter-critical heat treatment with a second peak temperature of 735 °C

	YS (MPa)	UTS (MPa)	YS/UTS
Reference material	347	575	0.60
Variant I	404	592	0.68
Variant II	592	732	0.79
Variant III	532	667	0.79

allow to increase the mechanical strength while maintaining a ratio between yield strength and maximum load YS/UTS (lower than 0.8). In addition, there is a beneficial effect of the addition of vanadium on fatigue resistance, especially in conditions of low number of cycles to rupture (*e.g.,* cranes, wind towers).

Conclusion

In this work, the effect of the alloying of vanadium on an S355 steel grade subjected to a double-pass welding thermal cycle, with the second peak temperature in the inter-critical zone, was studied. Four steel variants with different vanadium contents were taken into account and, for each of these, the IC GC HAZ area was simulated by dilatometer and Gleeble, investigating five different inter-critical temperatures of the secondary peak (between 720 and 790 °C). Following the heat treatment, microstructural investigations (microstructural constituent variation, RA formation, and precipitation state) and mechanical performance tests were conducted.

The results can be summarized as follows:

- The addition of vanadium does not provide a significant influence on the microstructural variation. As the inter-critical temperature increases, the microstructure varies from bainite to ferrite-pearlite, regardless of the chemical composition considered.
- Vanadium addition was found to favor the formation of RA; however, the amount of RA formed was not significant enough to induce detrimental effects on fatigue resistance (less than 0.6%).
- Adding vanadium promotes the formation of fine precipitates in the IC GC HAZ. The variant with a higher content of vanadium (0.10 wt%) exhibited V-rich precipitates with a size smaller than 60 nm, of which more than 50% were smaller than 15 nm. This evidence does not appear critical in terms of fatigue strength, as would be expected for larger precipitates.
- The variant with the highest vanadium content (0.10 wt%) presents an increase in static mechanical resistance, associated with an improvement in fatigue performance, mainly in conditions of low number of cycles to rupture.

Declarations

Conflict of interest The authors declare no conflict of interest.

References

1. F. Fazeli, B.S. Amirkhiz, C. Scott, M. Arafin, L. Collins, Mater. Sci. Eng. A (2018). https://doi.org/10.1016/j.msea.2018.02.042
2. A. Di Schino, M. Gaggiotti, C. Testani, Metals (2020). https://doi.org/10.3390/met10060808
3. S. Mengaroni, F. Cianetti, M. Calderini, E. Evangelista, A. Di Schino, H. McQueen, Acta Phys. Pol. (2015). https://doi.org/10.12693/APhysPolA.128.629
4. A. Di Schino, C. Testani, Metals (2020). https://doi.org/10.3390/met10040552
5. G. Stornelli, A. Di Schino, S. Mancini, R. Montanari, C. Testani, A. Varone, Appl. Sci. (2021). https://doi.org/10.3390/app11221210598
6. A. Lambert-Perlade, A.F. Gourges, J. Besson, T. Sturel, A. Pineau, Metall. Mater. Trans. A (2004). https://doi.org/10.1007/s11661-004-0030-y
7. M. Narimani, E. Hajjari, M. Eskandari, J.A. Szpunar, J. Mater. Eng. Perform. (2022). https://doi.org/10.1007/s11665-021-06454-0
8. B.C. Kim, S. Lee, N.J. Kim, D.Y. Lee, Metall. Trans. A (1991). https://doi.org/10.1007/BF03350956
9. A. Di Schino, C. Guarnaschelli, Mater. Sci. Forum (2010). https://doi.org/10.4028/www.scientific.net/MSF.638-642.3188
10. G. Spanos, R.W. Fonda, R.A. Vandermeer, A. Matuszeski, Metall. Mater. Trans. A (1995). https://doi.org/10.1007/BF02669455
11. S. Lee, B.C. Kim, D. Kwon, Metall. Trans. A (1992). https://doi.org/10.1007/BF02651759
12. R. Taillard, P. Verrier, T. Maurickx, J. Foct, Metall. Mater. Trans. A (1995). https://doi.org/10.1007/BF02664681
13. J. Cui, W. Zhu, Z. Chen, L. Chen, Metall. Mater. Trans. A (2020). https://doi.org/10.1007/s11661-020-06017-3
14. Y. Li, D.N. Crowther, M.J.W. Green, P.S. Mitchell, T.N. Baker, ISIJ Intern. (2001). https://doi.org/10.2355/isijinternational.41.46
15. L. Cho, A. Tselikova, K. Holtgrewe, E. De Moor, R. Schmidt, K.O. Findley, Mater. Sci. Technol. (2022). https://doi.org/10.1080/02670836.2022.2088163
16. T. Kasuya, N. Yurioka, Weld. Res. Suppl. **72**, 263 (1993)
17. G. Stornelli, A. Tselikova, D. MirabileGattia, M. Mortello, R. Schmidt, M. Sgambetterra, C. Testani, G. Zucca, A. Di Schino, Materials (2023). https://doi.org/10.3390/ma16072897
18. M. Hajisafari, S. Nategh, H. Yoozbashizadeh, A. Ekrami, J. Mater. Eng. Perform. (2013). https://doi.org/10.1007/s11665-012-0324-y
19. A. Di Schino, J.M. Kenny, I. Salvatori, G. Abbruzzese, J. Mat. Sci. (2001). https://doi.org/10.1023/A:1004856001632
20. G. Stornelli, M. Gaggiotti, D. MirabileGattia, R. Schmidt, M. Sgambetterra, A. Tselikova, G. Zucca, A. Di Schino, Acta Metall. Slov. (2022). https://doi.org/10.36547/ams.28.3.1535
21. J.M. Rodriguez-Ibabe, Mater. Sci. Forum (1998). https://doi.org/10.4028/www.scientific.net/MS.284-286.51
22. E.V. Avtokratova, O. Sitdikov, O.E. Latypova, M.V. Markushev, M.L. Linderov, D.L. Merson, Y.A. Vinogradov, IOP Conf. Ser. Mater. Sci. Eng. (2018). https://doi.org/10.1088/1757-899X/447/1/012038
23. A. Di Schino, M. Barteri, J.M. Kenny, J. Mater. Sci. Lett. (2003). https://doi.org/10.1023/A:1026155215111